Molecular Therapy
Oncolytics
Original Article

Chimeric anti-GPC3 sFv-CD3ε receptor-modified T cells with IL7 co-expression for the treatment of solid tumors

Yansha Sun,[1,4] Yiwei Dong,[1,4] Ruixin Sun,[1] Yifan Liu,[1] Yi Wang,[2] Hong Luo,[3] Bizhi Shi,[2] Hua Jiang,[1,2] and Zonghai Li[1,2]

[1]State Key Laboratory of Oncogenes and Related Genes, Shanghai Cancer Institute, Renji Hospital, Shanghai Jiaotong University School of Medicine, Shanghai 200032, China; [2]CARsgen Therapeutics, Shanghai 200032, China; [3]State Key Laboratory of Oncogenes and Related Genes, Shanghai Cancer Institute, Renji Hospital, School of Biomedical Engineering, Shanghai Jiaotong University, Shanghai 200032, China

Chimeric antigen receptor (CAR) T cells targeting glypican-3 (GPC3) demonstrated early signs of therapeutic efficacy to hepatocellular carcinoma patients with a risk of cytokine release syndrome (CRS). Several adoptive cell therapies (ACTs) with T cells using the natural T cell receptor (TCR) signaling induced more efficient antitumor function and reduced cytokine production relative to CARs in solid tumors. To improve the efficacy and safety of GPC3-targeted ACTs, T cells were modified with anti-GPC3 single-chain fragment variable(sFv) linked to CD3ε, which could be incorporated into the entire TCR/CD3 complex to form chimeric sFv-CD3ε receptor (sFv-ε). sFv-ε T cells showed competitive antitumor activity and lower cytokine release compared to 28ζ or BBζ CAR T cells, which may be ascribed to moderately less activated Ca^{2+}-calcineurin-NFAT signaling pathway. We further generated murine sFv-ε T cells with interleukin-7 co-expression (7sFv-ε) to promote T cell survival and to mobilize the endogenous immune system. In immunocompetent mouse models, 7sFv-ε T cells showed superior persistence, antitumor efficacy, and immunological memory while preserving the low production of cytokines associated with CRS compared to conventional sFv-ε T cells. These results indicate that GPC3-specific 7sFv-ε T cells could serve as a promising therapeutic strategy for solid tumors.

INTRODUCTION

Improved understanding of tumor immunity over the past decades has led to the accelerated development of adoptive cell therapies (ACTs), including autologous tumor-infiltrating lymphocytes (TILs), T cell receptor (TCR), and chimeric antigen receptor (CAR) engineered T cells. TCR and CAR T cells are generated by modifying peripheral T cells to express a precisely defined antigen-specific receptor. TCR T cells recognize antigenic peptides presented on major histocompatibility complex (MHC) molecules, the function of which may be impaired by reduced or absent MHC on tumor cells or disruption of antigen processing and presentation, and was constrained to patients with a particular MHC allele.[1,2] In contrast, CARs containing an extracellular antigen-binding domain, mostly antibody-derived single-chain fragment variable (sFv), could successfully target antigens on tumor cells in an MHC-independent fashion.[3] For second-generation CARs, the co-stimulatory signaling domain (e.g., CD28, 4-1BB) and the intracellular region of CD3ζ subunit were included to recapitulate signals of T cell activation.[4,5]

Several CAR T cell therapies targeting CD19 or B cell mature antigen have been approved for hematological malignancies and produced impressive clinical responses with a high incidence of any-grade cytokine release syndrome (CRS).[6–12] For solid tumors, therapeutic effects have been reported in a limited number of patients treated with CAR T cells in most studies.[13–15] TILs or TCR T cells that rely on TCR signaling have shown encouraging antitumor activity in melanoma and synovial cell carcinoma with lower frequency and severity of adverse events compared with CAR T cells, suggesting chimeric TCR exploiting natural TCR signaling may be a strategy to induce better efficacy with reduced cytokine release.[16–18] In 1999, Nolan et al. noted that sFv directly fused to CD3ε could also redirect T cells to antigen targets in an MHC-unrestricted manner but the surface expression of sFv-ε required other endogenous TCR subunits, and they suggested linking sFv and CD3ε with an additional spacer to enhance the recognition to cellular antigen.[19] Glypican-3 (GPC3), a membrane-bound heparin sulfate proteoglycan, is overexpressed in several solid tumors, most notably in 70%–80% of hepatocellular carcinomas (HCCs), but rarely expressed in healthy adult tissues, making it a promising target for immunotherapy.[20,21]

Received 8 December 2021; accepted 14 April 2022;
https://doi.org/10.1016/j.omto.2022.04.003.

[4]These authors contributed equally

Correspondence: Hua Jiang, State Key Laboratory of Oncogenes and Related Genes, Shanghai Cancer Institute, Renji Hospital, Shanghai Jiaotong University School of Medicine, No. 25/Ln2200 XieTu Road, Shanghai 200032, China.
E-mail: jianghuapy@163.com
Correspondence: Zonghai Li, State Key Laboratory of Oncogenes and Related Genes, Shanghai Cancer Institute, Renji Hospital, Shanghai Jiaotong University School of Medicine, No. 25/Ln2200 XieTu Road, Shanghai 200032, China.
E-mail: zonghaili@shsmu.edu.cn

This is an open access article under the CC BY-NC-ND license (http://creativecommons.org/licenses/by-nc-nd/4.0/).

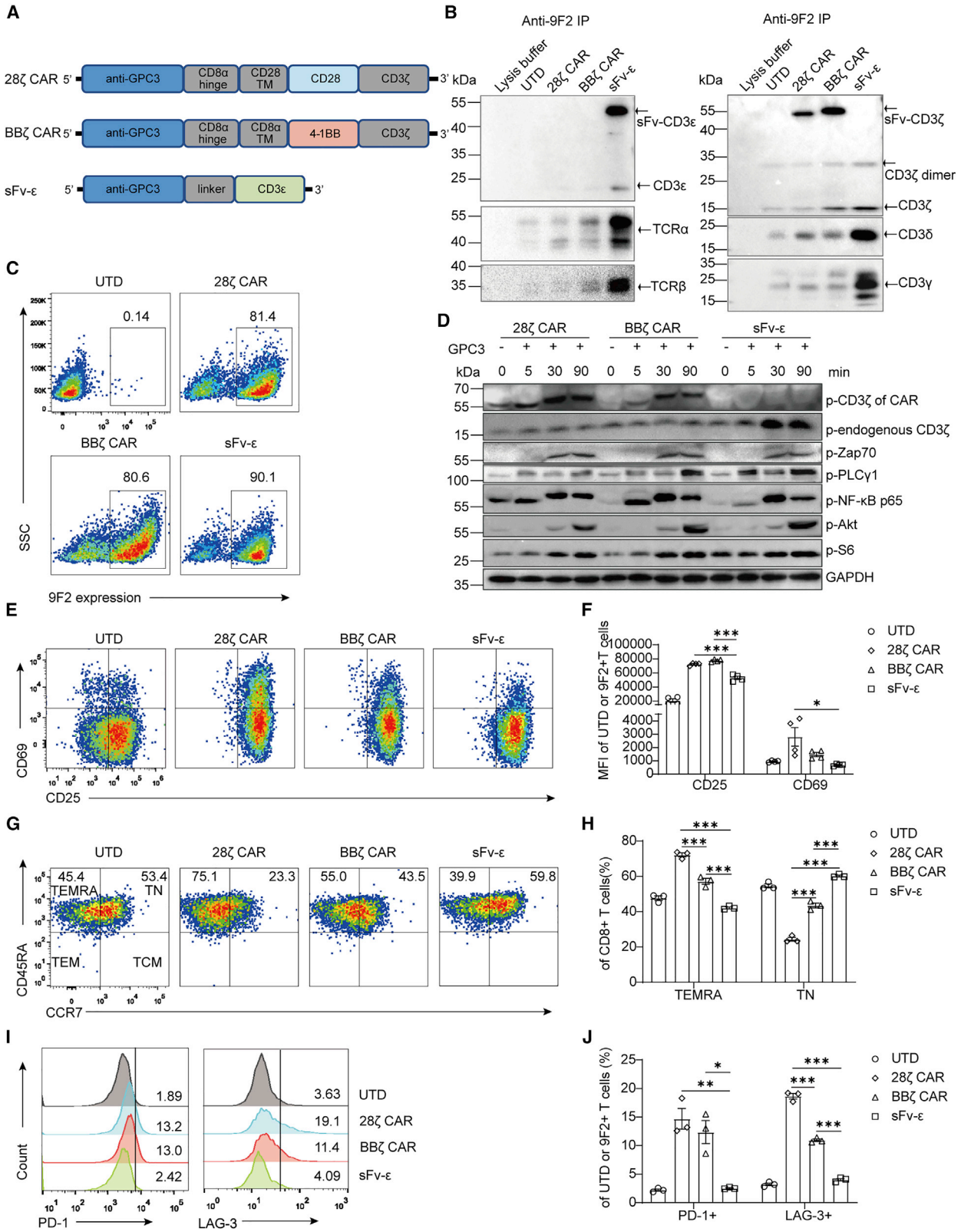

(legend on next page)

Our clinical trials suggested early signs of antitumor response of GPC3-specific 28ζ CAR T cells to advanced HCCs, but 8 of 13 patients experienced grade 1 or 2 CRS and 1 patient suffered grade 5 CRS (NCT02395250, NCT03146234).[22] To improve the safety and applicability of GPC3-targeted T cell therapy, we genetically modified T cells with anti-GPC3 sFv linked to CD3ε, which should be incorporated into the TCR/CD3 complex. The resulting complex is considered achimeric sFv-ε TCR in nature and should mimic TCR signaling independent of MHC. In the functional immune system, the hostile tumor microenvironment could impair the persistence and effector function of adoptive transferred T cells, but tumor-primed host T cells may provide protective memory against tumor relapse.[23,24] Interleukin-7 (IL7) functions as a survival-promoting factor for cytotoxic T lymphocytes (CTLs) and memory T cells, which produced synergistic antitumor effects with ACTs.[25–28] Therefore, we generated sFv-ε T cells constitutively expressing interleukin-7 (7sFv-ε) and evaluated its antitumor activities in preclinical mouse models.

RESULTS

Human sFv-ε T cells had TCR-like signaling with alleviated auto-activation compared to CAR T cells

The human sFv-ε expressing construct was synthesized by fusing the anti-GPC3 sFv (9F2) and the CD3ε via a linker. The same 9F2 was used for constructions of 28ζ and BBζ CAR. Main elements of lentiviral vectors encoding sFv-ε or CAR were illustrated in Figure 1A. To investigate whether the sFv-CD3ε could be incorporated into the human TCR, Jurkat cells stably expressing sFv-ε or CAR were established (Figure S1). A co-immunoprecipitation assay revealed that all of the endogenous TCR subunits (including TCRα, TCRβ, CD3ζ, CD3ε, CD3δ, and CD3γ) evidently bound with sFv-ε but barely with CAR (Figure 1B). This indicated that sFv-ε could form an intact TCR/CD3 complex distinct from CARs, which use an isolated CD3ζ signaling domain.

To explore whether sFv-ε could mediate TCR-like signaling, we generated anti-GPC3 sFv-ε T or CAR T cells using primary human T cells. The sFv-ε T and CAR T cells presented approximately equal proportions of T cells with 9F2 expression (Figure 1C). Untransduced (UTD) T cells served as control. Next, we evaluated the phosphorylation kinetics and duration of key TCR signaling molecules in sFv-ε T or CAR T cells when activated with GPC3 peptide. TCR signaling is initiated by Lck-mediated phosphorylation of immunoreceptor tyrosine activation motifs within the cytoplasmic domain of CD3 subunits. As shown in Figure 1D, in the absence of antigen, sFv-ε T and CAR T cells showed similar basal phosphorylation of endogenous CD3ζ while CAR T cells demonstrated additional constitutive phosphorylation of CAR-derived CD3ζ. Upon antigen stimulation, sFv-ε but not CARs induced the phosphorylation of endogenous CD3ζ, which implied that sFv-ε could transduce antigen activation through the entire TCR/CD3 complex. Then, sFv-ε and CARs shared similar proximal signaling events, including the phosphorylation of Zap-70 and PLCγ1 (Figure 1D). For the distal TCR signaling pathways, both 28ζ and BBζ CAR T cells showed earlier and stronger phosphorylation of nuclear factor κB (NF-κB) p65 than sFv-ε T cells (Figure 1D). sFv-ε induced comparable phosphorylation levels of Akt and ribosomal protein S6, a downstream effector of the mammalian target of rapamycin (mTOR), to 28ζ and BBζ CARs after antigen stimulation for 30 or 90 min (Figure 1D).

Under normal culture conditions, 28ζ and BBζ CAR T cells expressed higher CD25 and CD69 than sFv-ε and UTD T cells, indicating their prolonged auto-activation (Figures 1E and 1F). We further analyzed whether the tonic signaling would facilitate T cell differentiation and exhaustion.[29,30] The proportion of terminally differentiated effector memory T cells (TEMRA), presented as CD45RA + $CCR7^{-}$ subsets of CD8+ T cells, is enriched in 28ζ and BBζ CAR T cells, particularly in 28ζ CAR T cells. On the contrary, sFv-ε T cells preserved a less-differentiated naive phenotype, defined by CD45RA + $CCR7^{+}$ subsets of $CD8^{+}$ T cells (Figures 1G and 1H). 28ζ and BBζ CAR T cells also revealed a significant upregulation of immune exhaustion marker PD-1 and LAG-3 compared to sFv-ε T cells (Figures 1I and 1J). These results suggested that sFv-ε significantly attenuated tonic signaling compared to CARs.

Human sFv-ε T cells showed competitive antitumor efficacy with reduced cytokine production

To examine whether antigen-activated sFv-ε T cells can mediate cytolytic effector functions, sFv-ε T or CAR T cells were cocultured with human HCC cell lines PLC/PRF/5 or SK-Hep-1 (Figure S2A). All of the engineered T cells exhibited equipotent cytotoxicity against GPC3-expressing PLC/PRF/5 cells in an effector-to-target ratio-dependent manner but barely had cytotoxicity to GPC3-negative SK-Hep-1 cells (Figure 2A). CRS associated with CAR T cell therapy is characterized by elevated peripheral cytokines, including IL6, interferon γ (IFNγ), tumor necrosis factor α (TNFα), IL2, and granulocyte macrophage-colony stimulating factor (GM-CSF). Monocytes were reported to be the major source of IL6 in CRS.[31] Thus, we set up an *in vitro* cytokine release assay, in which T cells were incubated with PLC/PRF/5 cells with or without primary autologous monocytes. The results showed

Figure 1. Distinct signatures of activation, differentiation, and inhibition phenotype in human 28ζ CAR, BBζ CAR, and sFv-ε T cells

(A) Schematic diagram of the encoding sequence of anti-GPC3 sFv-ε and CARs. (B) Complex formation of sFv-CD3ε with TCR subunits. Upon Jurkat cell lysis, sFv-ε and CARs were immunopurified using the biotin-labeled GPC3 peptide and streptavidin-coupled beads, and separated by reducing SDS-PAGE and analyzed by western blot. The lysis buffer served as control. (C) Surface expression of sFv-ε and CARs on primary human T cells. (D) T cells were stimulated with GPC3 peptide and the phosphorylation of downstream proteins of TCR were analyzed by western blot. GAPDH served as internal control. (E and F) Surface expression of CD25 and CD69 of UTD or $9F2^{+}$ T cells (n = 4). (G and H) Frequencies of $CD45RA^{+}$ $CCR7^{+}$ naive (TN) and $CD45RA^{+}$ $CCR7^{-}$ terminally differentiated effector memory T cell (TEMRA) subsets in $CD8^{+}$ T cells (n = 3). (I and J) Surface expression of PD-1 and LAG-3 in UTD or $9F2^{+}$ T cells (n = 3). Each experiment was repeated at least 3 times independently with similar results, and representative data are shown. Data are represented as means ± SEMs. Statistical analysis was performed using parametric one-way ANOVA followed by Tukey's test comparing all of the engineered T cell groups against one another (F, H, and J). *Adjusted $p \leq 0.05$, **adjusted $p \leq 0.01$, ***adjusted $p \leq 0.001$.

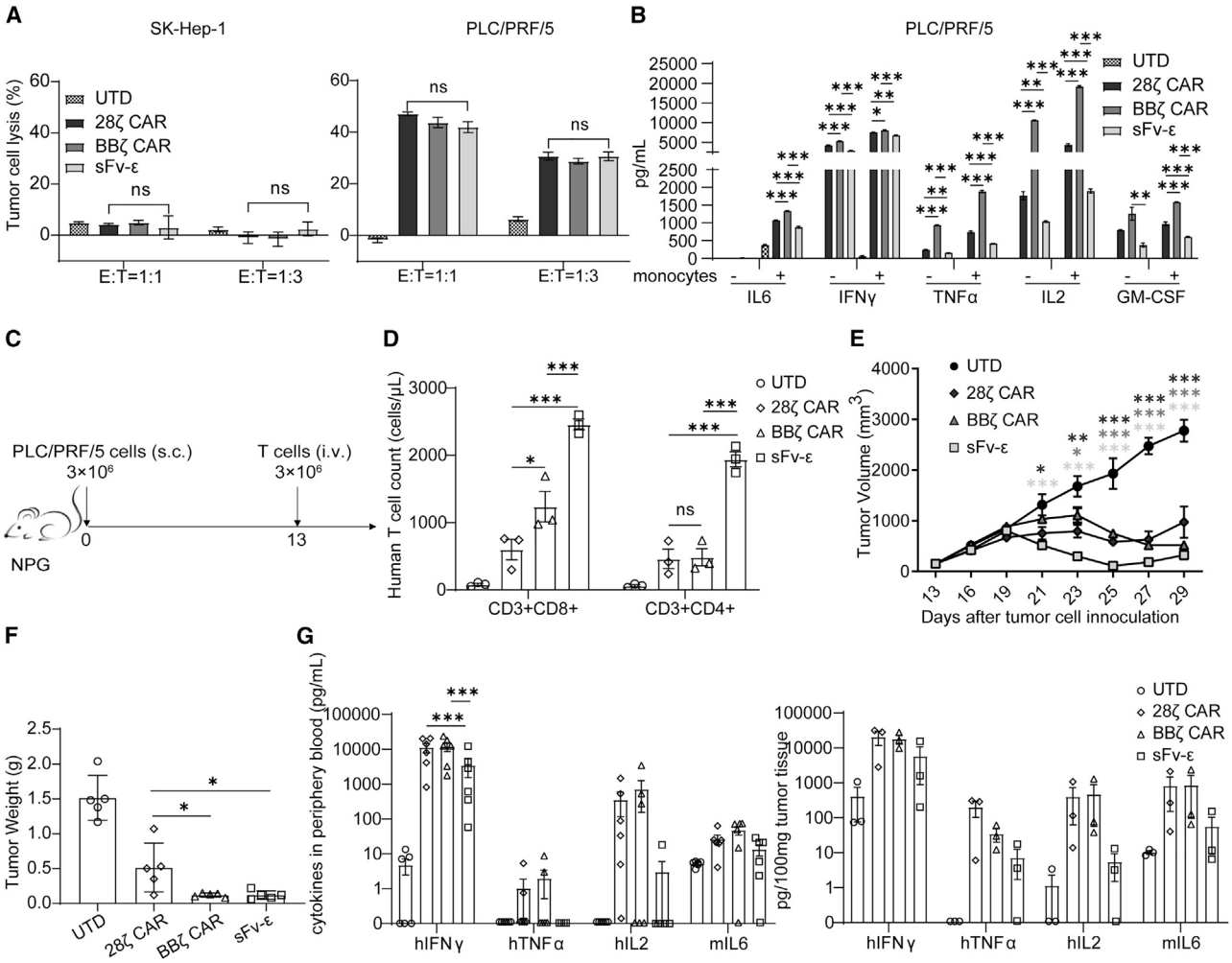

Figure 2. Characterization of antitumor activity and cytokine production of human 28ζ CAR, BBζ CAR, and sFv-ε T cells

(A) T cells were co-incubated with SK-Hep-1 or PLC/PRF/5 tumor cells at the indicated effector to target (E:T) ratios for 18 h (n = 3–4). Cytotoxic activities were measured using a standard nonradioactive cytotoxicity assay. (B) T cells were cocultured with PLC/PRF/5 cells with or without monocytes at the ratio of 1:1:1 or 1:1:0 for 48 h. IL6, IFNγ, TNFα, and IL2 in co-culture supernatants were quantified by cytometric bead array (CBA) assays, and GM-CSF was examined by ELISA (n = 3). (C) Experimental scheme in PLC/PRF/5 models. PLC/PRF/5 tumor cells 3×10^6 were subcutaneously injected into NPG mice on day 0. On day 13, mice bearing tumors of ~155 mm^3 were treated with a single intravenous infusion of 3×10^6 T cells. (D) $CD3^+CD8^+$ and $CD3^+CD4^+$ T cells in peripheral blood were measured with Trucount tubes 7 days after treatment (n = 3). (E) Growth of PLC/PRF/5 xenografts were monitored over 29 days (n = 5). (F) Tumor weights at the end of the experiment (n = 5). (G) Tumor-bearing mice were intravenously infused with 1.5×10^7 $9F2^+$ or UTD T cells. Human IFNγ, TNFα, IL2, and murine IL6 in peripheral blood were measured 3 and 6 days after treatment (n = 6 from 3 different mice of each group). Cytokines were also measured in tumor tissues harvested 6 days after treatment (n = 3). Measurements that fall below the limit of detection are defined as 0 and depicted on the x axis of the graph. Data are represented as means ± SEMs. Statistical analysis was performed using one-way ANOVA followed by Tukey's (A, B, D, F, G) or Dunnett's (E) test comparing engineered T cell groups against each other (A, B, D, F, G) or engineered T cell groups to UTD T cell group (E). ns, not significant, *adjusted $p \leq 0.05$, **adjusted $p \leq 0.01$, ***adjusted $p \leq 0.001$.

that sFv-ε T cells generally induced less secretion of IL6, IFNγ, TNFα, IL2, and GM-CSF than did CAR T cells (Figure 2B).

The *in vivo* antitumor efficacy of sFv-ε and CAR T cells were further evaluated in PLC/PRF/5 tumor-bearing mice (Figure 2C). The sFv-ε T group displayed enhanced persistence of $CD4^+$ and $CD8^+$ T cells in peripheral blood in comparison to 28ζ and BBζ CAR T groups 7 days after T cell infusion (Figure 2D). sFv-ε T cells induced superior tumor regression to CAR T cells at the early stage (Figure 2E). At the end of this experiment, sFv-ε T cells or BBζ CAR T cells suppressed tumor growth more effectively than did 28ζ CAR T cells (Figure 2F). All of the treatments did not affect body weight growth, and the pathologic analysis showed no adverse effects on normal internal organs (Figures S2B and S2C). In another experiment, cytokines in tumor-bearing mice receiving increased amounts of T cells were examined. There was a tendency toward less human IFNγ, TNFα, IL2, and

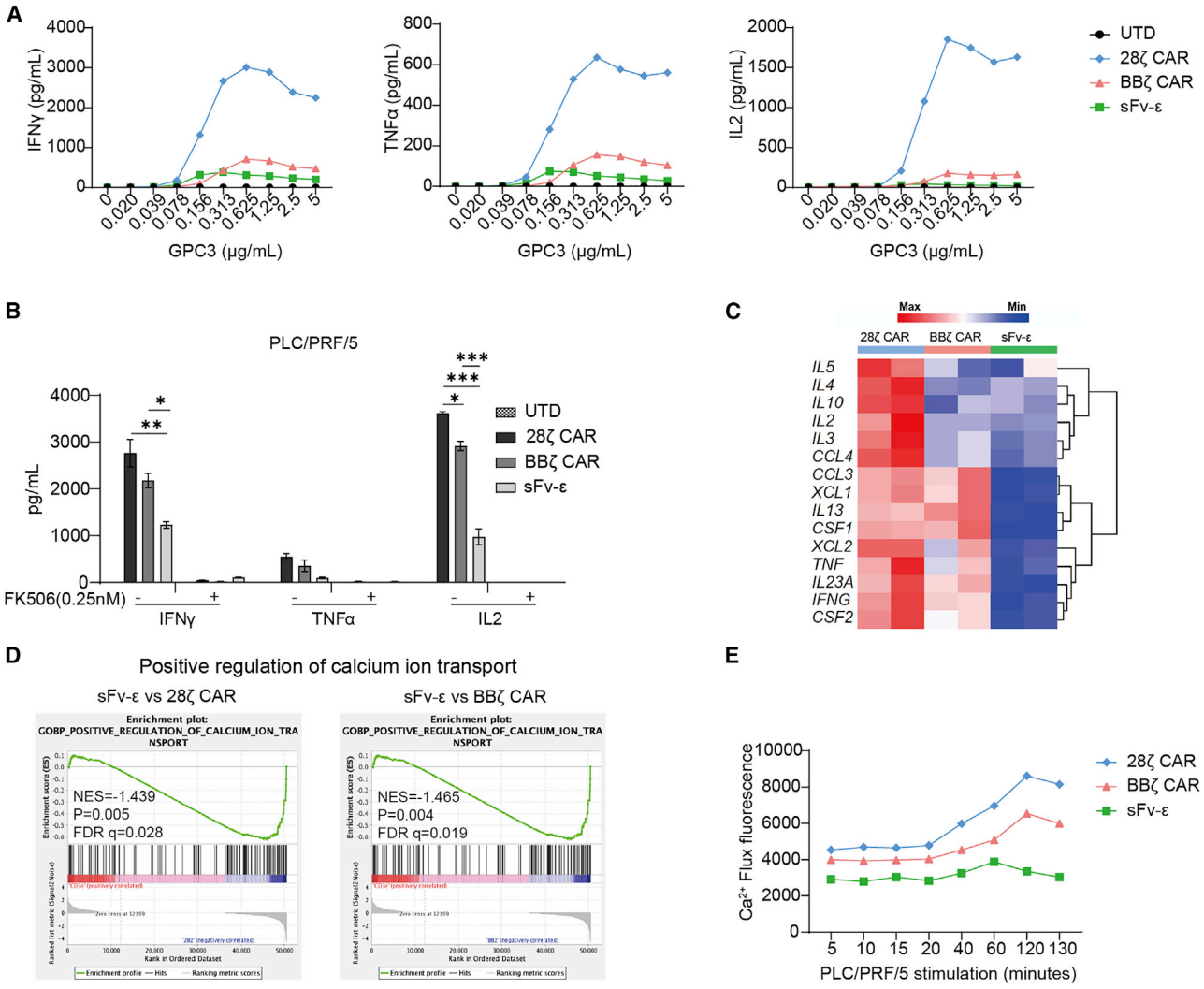

Figure 3. Characterization of sFv-ε or CAR-mediated calcium-calcineurin-NFAT signaling

(A) T cells were stimulated with GPC3 peptide of gradient concentrations for 8 h, and the cytokines in supernatants were quantified. Representative data are shown. (B) T cells were co-incubated with PLC/PRF/5 cells at a 1:1 ratio with or without calcineurin inhibitor FK506 (0.25 nM) for 8 h, and the cytokines in supernatants were measured (n = 3). (C) RNA sequencing was performed on T cells stimulated with immobilized GPC3 peptide for 4 h (n = 2). The heatmap shows NFAT-regulated gene expression, with red and blue representing higher and lower transcription, respectively. (D) GSEA of the positive regulation of calcium ion transport between sFv-ε T and 28ζ CAR T cells or between sFv-ε T and BBζ CAR T cells. (E) The intracellular calcium level of sFv-ε or CAR T cells stimulated with PLC/PRF/5 cells were analyzed by flow cytometry. Representative data are shown. Data are represented as means ± SEMs. Statistical analysis was performed using one-way ANOVA followed by Tukey's test comparing engineered T cell groups against each other (B). *Adjusted $p \leq 0.05$, **adjusted $p \leq 0.01$, ***adjusted $p \leq 0.001$.

mouse IL6 in peripheral blood and tumor tissues of sFv-ε T cell-treated mice than that of CAR T cell-treated mice (Figure 2G). These data revealed that human GPC3-specific sFv-ε T cells can mediate competitive antitumor efficacy with CAR T cells while reducing the production of some cytokines associated with CRS.

sFv-ε mediated weaker calcium-calcineurin-nuclear factor of activated T cells (NFAT) signaling than CAR

We next tried to investigate the signaling basis of reduced cytokine production of sFv-ε T cells. Gradient concentrations of GPC3 peptide were used to activate T cells, which would provide antigen-induced signaling with distinct intensities. The results showed that sFv-ε T cells secreted less IFNγ, TNFα, and IL2 than CAR T cells after stimulation with 0.313μg/mL or higher amounts of antigen for 8 h (Figure 3A). Similarly, the lowest level of IFNγ, TNFα, and IL2 release was observed in sFv-ε T cells when different engineered T cells were cocultured with PLC/PRF/5 cells for 8 h (Figure 3B). To explore whether sFv-ε or CAR signaling regulates cytokine transcription differently, T cells stimulated with high levels of GPC3 peptide were subjected to transcriptome analysis. As shown in Figure 3C, the

mRNA expression levels of many NFAT-regulated cytokines were decreased in sFv-ε T cells compared to 28ζ or BBζ CAR T cells, including IFNγ, TNFα, IL2, and GM-CSF. The calcium/calcineurin/NFAT network plays an important role in cytokine production. The increase in intracellular Ca^{2+} leads to the rapid activation of calcineurin that causes NFAT dephosphorylation, nuclear translocation, and consequent gene transcription.[32,33] In addition, the calcineurin inhibitor FK506 almost abolished the production of IFNγ, TNFα, and IL2 by all of the engineered T cells, indicating that these cytokines were regulated mainly by the calcineurin-NFAT pathway (Figure 3B).[34] Gene set enrichment analysis (GSEA) revealed that the positive regulation of calcium ion transport was less active in sFv-ε T cells than that in CAR T cells (Figure 3D). Thus, the intracellular Ca^{2+} levels in human sFv-ε and CAR T cells were further analyzed upon coculture with PLC/PRF/5 cells. The increasing amplitude and duration of Ca^{2+} in sFv-ε T cells were inferior to that in CAR T cells (Figure 3E). These findings suggested that lower activation of the calcium-calcineurin-NFAT pathway in sFv-ε T than that in CAR T cells may contribute to the reduced production of IFNγ, TNFα, and IL2.

Co-expression of IL7 improved survival of murine 7sFv-ε T cells *in vitro*

To evaluate the different engineered T cells in immunocompetent models, expressing vectors for murine sFv-ε, 28ζ and BBζ CAR were generated (Figure 4A). In an attempt to promote T cell survival and immunological memory, we constructed murine sFv-ε co-expressing IL7 by fusing the sFv-ε and IL7 with a 2A peptide sequence, which was called 7sFv-ε (Figure 4A). Splenic T cells from C57BL/6 mice were transduced with respective retroviruses to generate sFv-ε, 7sFv-ε, or CAR T cells (Figure S3A). Considering that 9F2 recognizes human GPC3, we established murine hepatocellular carcinoma Hepa 1–6 and triple-negative breast cancer E0771 cell lines that express human-mouse chimeric GPC3 (Figure S3B).[35] 7sFv-ε T cells produced IL7 spontaneously and increased IL7 secretion when stimulated with tumor cells (Figure 4B). The memory differentiation and exhaustion phenotypes of murine T cells were analyzed. sFv-ε and 7sFv-ε T cells possessed a higher proportion of $CD44^+$ $CD62L^+$ central memory T cells than 28ζ and BBζ CAR T cells (Figures 4C and 4D). sFv-ε and 7sFv-ε T cells showed a significantly decreased expression of PD-1 and LAG-3 compared to CAR T cells (Figures 4E and 4F). To assess the susceptibility of T cells to IL2 deprivation-induced apoptosis, T cells were incubated without the addition of IL2 for 24 h. As expected, the percentage of apoptotic 7sFv-ε T cells was significantly lower than that of other engineered T cells (Figures 4G and 4H). The apoptosis-related proteins were analyzed by western blot. The results illustrate that in comparison to other engineered T cells, 7sFv-ε T cells had reduced caspase 3 activation accompanied by the upregulation of anti-apoptotic Mcl-1, Bcl-xL, and Survivin (Figure 4I). Moreover, in *in vitro* culture at low concentration of IL2, 7sFv-ε T cells exhibited improved proliferation relative to conventional sFv-ε T cells (Figure S3C).

7sFv-ε T cells displayed superior *in vivo* antitumor efficacy

The *in vitro* cytotoxicity studies demonstrated that all engineered T cells could specifically lyse GPC3-positive tumor cells with similar efficiency but not the parental GPC3-negative cell lines (Figure 5A). After co-culture with target cells, both sFv-ε and 7sFv-ε T cells secreted similar IFNγ but less TNFα, IL2, and GM-CSF than 28ζ and BBζ CAR T cells, and the co-expression of IL7 did not affect cytokine release *in vitro* (Figure 5B).

The *in vivo* antitumor activities of murine engineered T cells were first evaluated in Hepa 1-6-GPC3 models, which is immunologically responsive (Figure 5C). Conventional sFv-ε and 28ζ CAR T cells suppressed tumor growth and prolonged mice survival comparably, while BBζ CAR T cells lost the capacity to inhibit tumor growth earlier in 3 of 6 mice (Figures 5D and 5E). 7sFv-ε T cells led to complete tumor eradication in 4 of 6 mice after 40 days of treatment and remarkably improved the survival of mice compared to other engineered T cells (Figures 5D and 5E, median survival of different groups: 7sFv-ε, not reached; sFv-ε, 46.5 days; 28ζ CAR, 43 days; BBζ CAR, 39.5 days; UTD, 32.5 days). Their therapeutic effects were studied further in orthotopic E0771-GPC3 models, since GPC3 overexpression has also been seen in breast cancer and the E0771 model was reported to own an immunosuppressive microenvironment (Figure 5F).[21,36] Unfortunately, in comparison to UTD T cells, conventional sFv-ε T and CAR T cells failed to control tumor progression (Figures 5G and 5H). However, 7sFv-ε T cells still exhibited faster antitumor effect than others and almost completely eradicate the tumor eventually (Figures 5G and 5H). All of the adoptive T cell therapies did not affect body weight and no pathologic damage was observed in normal internal organs (Figures S4A–S4C). Cytokine release was further examined in Hepa 1-6-GPC3 models. In peripheral blood, sFv-ε and 7sFv-ε T cells produced or elicited lower level of IFNγ, TNFα and IL6 than BBζ CAR T cells did (Figure 5I). In tumor tissues, we observed a trend toward less IFNγ and TNFα production in sFv-ε and 7sFv-ε T cell groups than that in CAR T cell groups (Figure 5I). These data suggested that sFv-ε and 7sFv-ε T cells may reduce the risk of CRS compared with CAR T cells in immunocompetent hosts.

Co-expression of IL7 improved the persistence of murine 7sFv-ε T cells and induced immunological memory *in vivo*

To elucidate the mechanism underlying the enhanced antitumor ability of 7sFv-ε T cells, we investigated the persistence of T cells in Hepa 1-6-GPC3 models. As shown in Figures 6A and 6B, there were more CD4+ T cells in tumors of 7sFv-ε and 28ζ CAR T group than that of sFv-ε and BBζ CAR T group. Administration of 7sFv-ε T cells increased accumulation of CD8+ T cells and 9F2+ T cells the most, followed by sFv-ε, 28ζ CAR and BBζ CAR T cells. The transduced gene copy number in 7sFv-ε T group was significantly higher than that in other engineered T cell groups (Figure 6C). Furthermore, the tumor-infiltrating CD8+ cells in 7sFv-ε T cell group demonstrated elevated expression of granzyme B, suggesting an augmented cytolytic capacity against tumors (Figures 6D and S5A). In addition, 7sFv-ε T cell-treated mice had the most 9F2+ T cell survival in spleen (Figures 6E and S5B). Given these findings, the improved antitumor ability of 7sFv-ε T cells should be at least partially ascribed to the increased persistence of infused T cells.

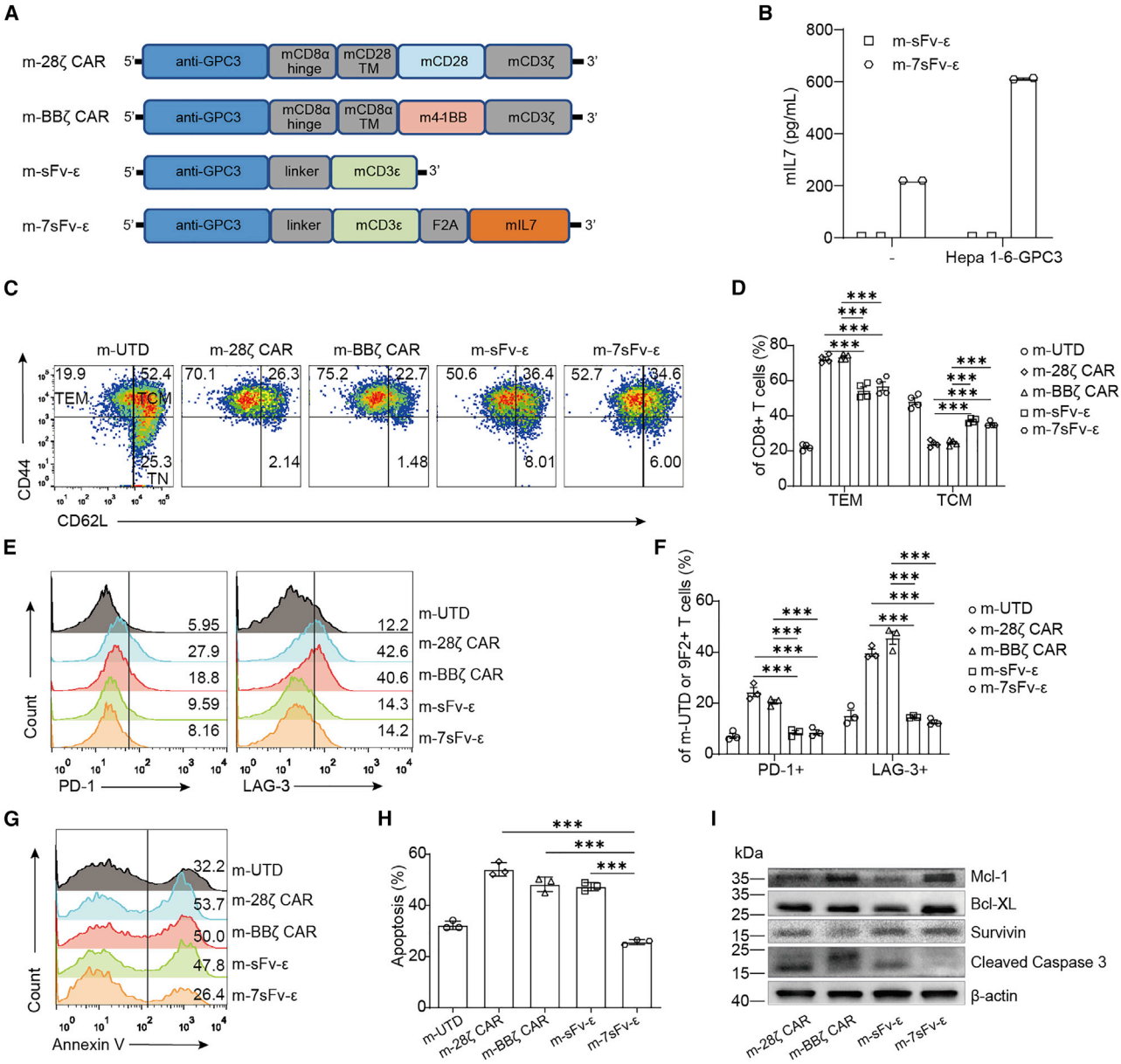

Figure 4. The function of IL7 on murine 7sFv-ε T cells *in vitro*

(A) Schematic diagram of the retroviral vector expressing murine anti-GPC3 sFv-ε, 7sFv-ε, and CARs. ("m" prefix denotes murine or mouse). (B) T cells were cultured with or without Hepa 1-6-GPC3 cells for 20 h. IL7 in the supernatant was analyzed by ELISA (n = 2). The conventional sFv-ε T cells were used as control. (C and D) Frequencies of $CD44^+$ $CD62L^+$ central memory (TCM) and $CD44^+$ CD62L-effector memory (TEM) subsets in $CD8^+$ T cells (n = 4). (E and F) Expression of PD-1 and LAG-3 in murine $9F2^+$ or UTD T cells (n = 3). (G and H) Frequencies of annexin V^+ cells in murine T cells following withdrawal of IL2 for 24 h (n = 3). (I) Expression of Mcl-1, Bcl-XL, Survivin, and Cleaved caspase 3 in murine engineered T cells following withdrawal of IL2 for 24 h were determined by western blot. β-actin were used as internal control. The experiments were repeated at least 3 times independently with similar results, and the representative data are shown. Data are represented as means ± SEMs. Statistical analysis was performed using one-way ANOVA followed by Tukey's (D and F) or Dunnett's (H) test comparing engineered T cell groups against one another (D and F) or all other engineered T cell groups to the 7sFv-ε T cell group (H). ***Adjusted $p \leq 0.001$.

Additionally, 7sFv-ε T cell treatment significantly promoted the CD8+ T cell proliferation and central memory T cell differentiation in the spleen and draining lymph nodes (Figures 6F–6I and S6A–S6F). Central memory T cells are supposed to be long-lived in secondary lymphoid organs and response to relapsed tumors more rapidly and effectively. Thus, after the primary tumors were removed by 7sFv-ε T cells, we re-injected Hepa 1-6-GPC3 cells in the contralateral flanks of mice (Figure 6J). Compared with naive mice, 7sFv-ε T cell-treated

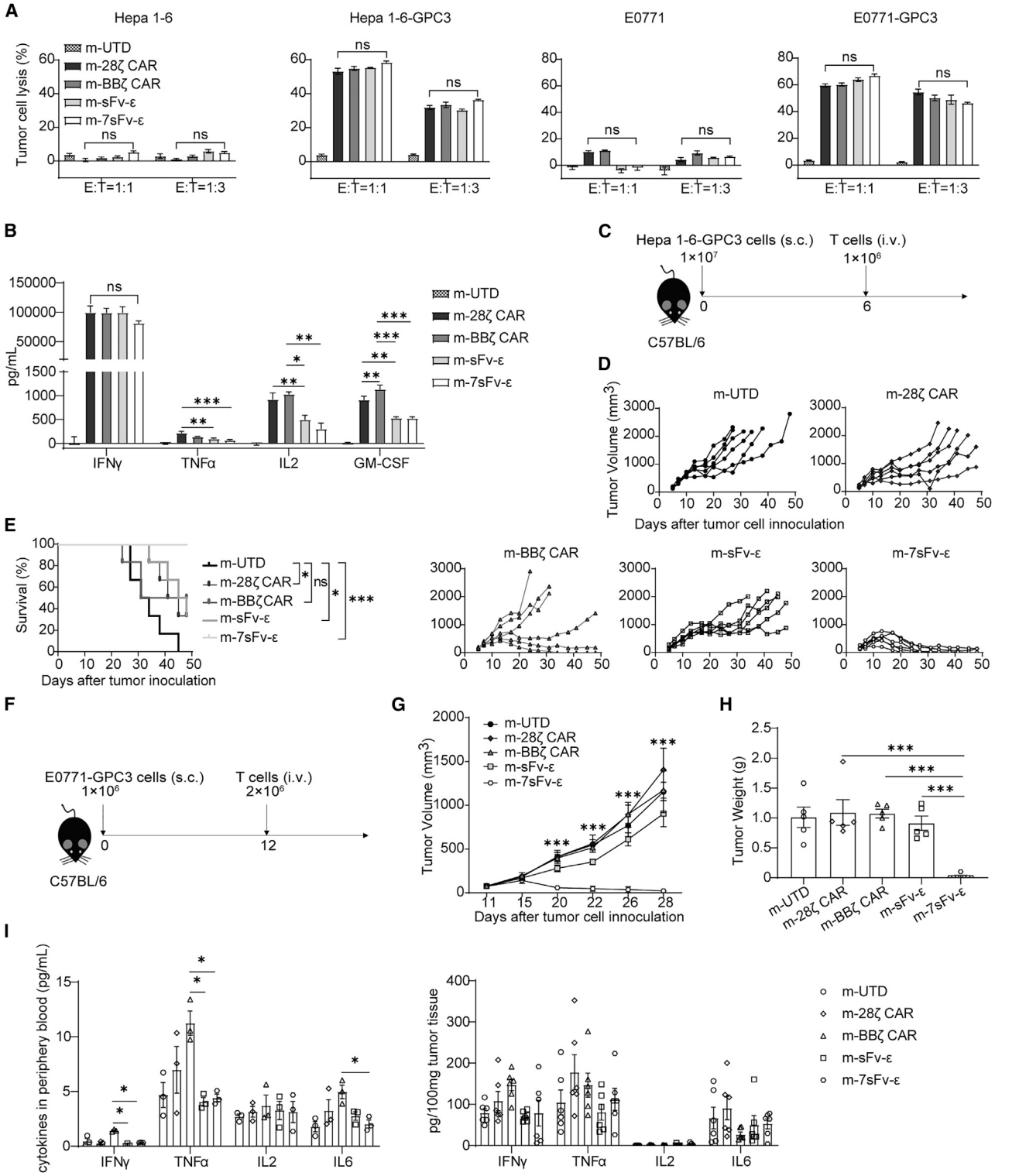

Figure 5. Characterization of antitumor activity and cytokine production of murine 28ζ CAR, BBζ CAR, sFv-ε, and 7sFv-ε T cells

(A) Murine T cells were co-incubated with parental and GPC3-overexpressing Hepa 1-6 and E0771 cells at varying effector:target (E:T) ratios for 18 h and the cytotoxic activities were measured (n = 3–4). (B) Murine T cells were co-incubated with Hepa 1-6-GPC3 cells at a 1:1 ratio for 20 h. IFNγ, TNFα, and IL2 in the supernatants were

(legend continued on next page)

mice showed immediate tumor elimination in all 6 mice that lasted more than 4 weeks, suggesting that 7sFv-ε T cell therapy could provide long-term protection from tumor recurrence (Figure 6K).

DISCUSSION

To improve the efficacy, safety, and availability of ACTs in solid tumors, various strategies have been proposed to redirect T cells to operate through the comprehensive TCR signaling in an MHC-unrestricted manner. T cells genetically equipped with T cell antigen coupler (TAC) containing a CD3ε recruitment domain have demonstrated more effective antitumor activity with lower cytokine production relative to CAR T cells.[37] Baeuerle et al. named and classified the designs characterized with an antibody-based binding domain fused to one of the TCR/CD3 subunits, including CD3ε as T cell receptor fusion constructs (TRuCs), and reported that compared to CAR T cells, ε-TRuC (sFv fused to ε) T cells showed improved antitumor effects in liquid tumor NSG (NOD.Cg-*Prkdc*^{scid} *Il2rg*^{tm1Wjl}/SzJ) mice xenograft models and less release of some cytokines *in vitro*.[38] In this study, we generated GPC3-specific sFv-ε and 7sFv-ε T cells and examined their properties in multiple solid tumor models in comparison with CAR T cells.

The sFv-ε construct was confirmed to integrate into the endogenous TCR/CD3 complex, and the recombinational sFv-ε could mediate the tyrosine phosphorylation of endogenous CD3ζ to activate several downstream pathways dependent on antigen. Under normal culture conditions, both human and murine sFv-ε T cells demonstrated alleviated auto-activation compared to 28ζ and BBζ CAR T cells, characterized by a higher proportion of naive or central memory subsets as well as less exhausted status, which could translate into longer survival of T cells and more efficient tumor killing *in vivo*.[39]

In immunodeficient mice inoculated with PLC/PRF/5 cells, sFv-ε T cells exhibited better survival at early stages and more rapid antitumor efficacy than CAR T cells. In Hepa 1-6-GPC3 models, the increased tumor infiltration of conventional sFv-ε T cells relative to CAR T cells was observed, which should contribute to the slightly prolonged survival of mice. However, approaches to further promote T cell persistence and mobilize the endogenous immune system are required to enhance therapeutic effects. IL7 signals through the heterodimeric IL7 receptor comprising IL7Rα and common cytokine receptor γ chain, which mediates anti-apoptotic and pro-proliferative effects. IL7Rα expression is maintained on naive and memory T cells and downregulated by IL7-mediated signaling and/or T cell activation to provide a built-in safety valve.[40] The clinical utilization of recombinant human IL7 (rhIL7) or CAR T cells secreting IL7 showed that IL7 is safe and well tolerated.[41,42] During the primary immune response, a minority of effector T cells re-express IL7Rα, suggesting that IL7 could instruct them to become memory cells.[43] The development of tumor-specific memory cells is helpful to prevent tumor recurrence.[24] In preclinical and clinical studies of solid tumors, IL7 presented vaccine adjuvant effects, and co-expression of IL7 could increase the antitumor activity of adoptive cell therapies.[27,28,42] The rhIL7 has convincingly shown potent T cell reconstitution effects through increasing naive T cell populations and TCR repertoire diversification.[44] IL7 may provide additional clinical benefits for cancer patients with immunodeficiency that commonly results from chemotherapy or old age. In our study, 7sFv-ε T cells that produce soluble IL7 promoted the survival of infused T cells and the differentiation of memory T cells, giving rise to the enhanced tumor suppression and reduced incidence of local tumor recurrence. The attenuated expression of IL7Ra in 7sFv-ε T cells supported a self-regulatory mechanism of IL7 signaling (Figure S3D). Regarding additional safety concerns, sFv-ε T cells can be engineered to inducibly express IL7, such as applying an NFAT-responsive promoter or a synNotch receptor.[45,46]

Previous studies have suggested that monocytes could be activated by T cells via either co-stimulatory receptors or T cell-derived cytokines, and then secrete cytokines to recruit and stimulate immune effectors to exacerbate CRS.[31,47] In our study, human sFv-ε T cells induced lower secretion of IL6, IFNγ, TNFα, IL2, and GM-CSF than CAR T cells when cocultured with tumor cells and monocytes *in vitro*. Murine sFv-ε and 7sFv-ε T cells released fewer cytokines, including TNFα, IL2, and GM-CSF than CAR T cells *in vitro*. The experiment using gradient concentrations of antigen suggested that there is a threshold and an appropriate range of antigen density for cytokine secretion, and the cytokine release patterns of sFv-ε and CAR T cells induced by higher antigen densities were in line with those activated with tumor cells. Upon high antigen stimulation, sFv-ε T cells had less transcription of NFAT target genes than CAR T cells, and sFv-ε T cells displayed lower Ca^{2+} influx than CAR T cells when cocultured with tumor cells. CTLs have a very low optimum intracellular Ca^{2+} for efficient cancer cell elimination.[48] The cytotoxicity is easier to trigger than cytokine production.[49] Thus, we deduce that the moderately less activated calcium-calcineurin-NFAT pathway in sFv-ε T cells is sufficient to

quantified by CBA (n = 4), and GM-CSF was examined by ELISA (n = 3). (C) Experimental scheme in Hepa 1-6-GPC3 models. Hepa 1-6-GPC3 cells 1×10^7 were injected subcutaneously into C57BL/6 mice on day 0. On day 6, mice bearing tumors of ~170 mm^3 were infused intravenously with 1×10^6 T cells. (D and E) The growth of Hepa 1-6-GPC3 allografts and survival of mice were monitored over 48 days (n = 6), with a tumor volume of 2,000 mm^3 or death as the endpoint. (F) Experimental scheme in E0771-GPC3 models. E0771-GPC3 cells 1×10^6 were injected *in situ* in the C57BL/6 mammary gland on day 0. On day 12, mice bearing tumors of ~100 mm^3 were infused with 2×10^6 T cells. (G) Growth of E0771-GPC3 allografts were monitored over 28 days (n = 5). (H) Tumor weights at the end of the experiment (n = 5). (I) In Hepa 1-6-GPC3 models, the peripheral blood was collected over 7 days (n = 3) and the tumor tissues were harvested ~10 days after treatment (n = 6). IFNγ, TNFα, IL2, and IL6 in peripheral blood and tumors were quantified by CBA. Measurements that fall below the limit of detection are defined as 0. Data are represented as means ± SEMs. Statistical analysis was performed using one-way ANOVA followed by Tukey's (A, B, H, I) or Dunnett's (G) test comparing engineered T cell groups against each other (A, B, H, I) or engineered T cell groups to the m-UTD T cell group (G). Survival curves were analyzed using the log rank (Mantel-Cox) test (E). ns, not significant, *adjusted $p \leq 0.05$, **adjusted $p \leq 0.01$, ***adjusted $p \leq 0.001$.

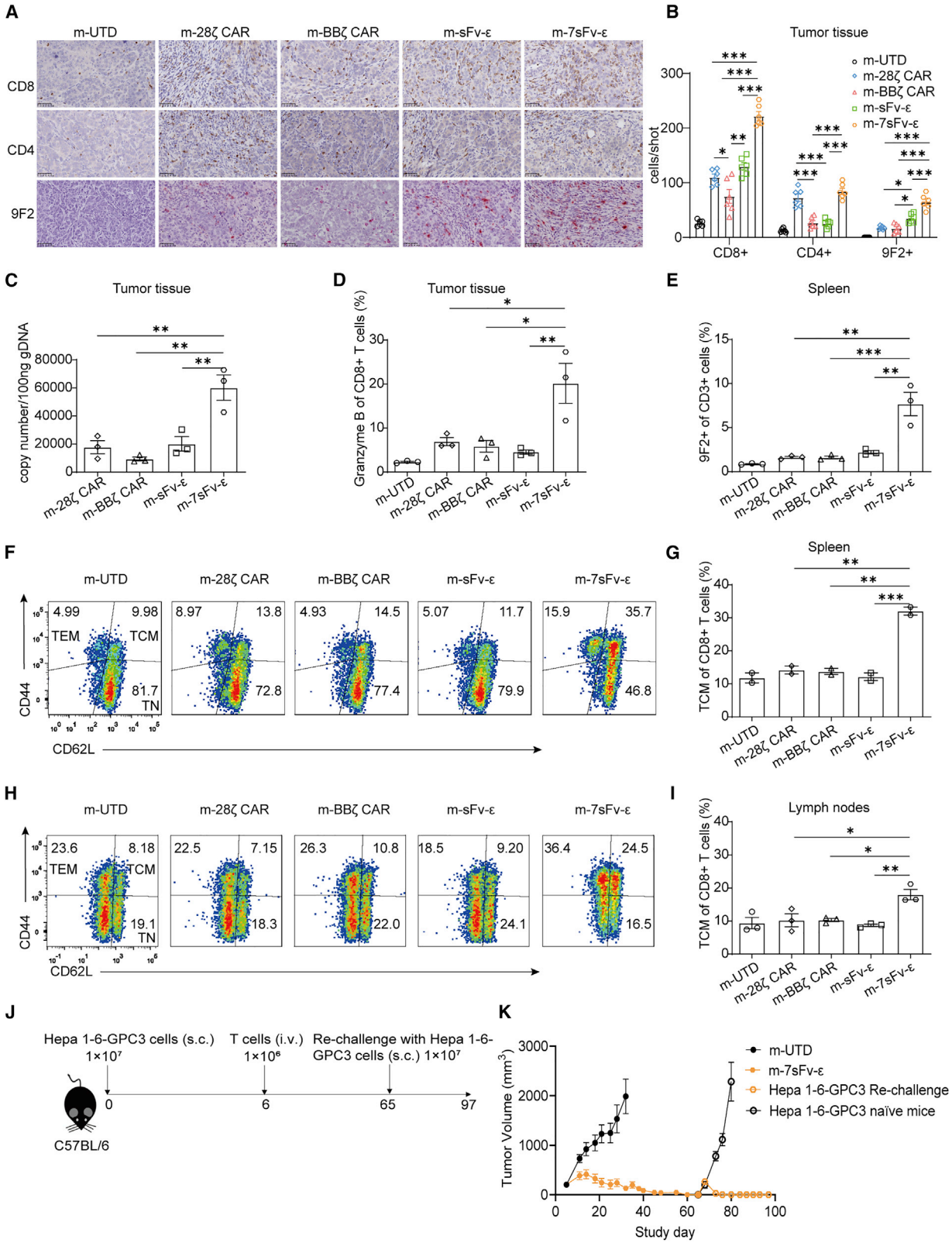

(legend on next page)

mediate antitumor effects despite decreasing cytokine production. Wu et al. reported that incorporation of CD3ε into 28ζ CAR could recruit Csk to attenuate CD3ζ/Zap70/PLCγ1 signaling and cytokine production.[50] In our study, sFv-ε, which is different from CAR in nature, did not exhibit reduced phosphorylation of Zap70 and PLCγ1 compared with 28ζ and BBζ CARs, implying that there are some other undefined regulatory mechanisms of the downstream calcium influx, which is worth exploring in the future.

Until now, major efforts were under way to develop appropriate animal models to reproduce CRS because the commonly established human tumor models in immunodeficient mice or syngeneic models in immunocompetent mice have limitations on describing the scenario occurring in patients with CRS. Giavridis et al. reported that 3×10^7 human CD19-specific 28ζ CAR T cells were used to elicit CRS in SCID-beige mice injected with Raji tumor cells intraperitoneally.[47] Norelli et al. established a novel xenotolerant mouse model that recapitulated severe CRS and lethal neurotoxicity induced by anti-CD19 CAR T cells in human.[31] Our study demonstrated that human sFv-ε T cells tended to induce less release of IFNγ, TNFα, IL2, and IL6 than CAR T cells in immunodeficient models, and among these, IL6 was from bystander cells. Murine sFv-ε and 7sFv-ε T cell therapies caused less IFNγ, TNFα, and IL6 secretion to peripheral blood relative to BBζ CAR T cell therapies. In the future, investigations of human sFv-ε and CAR T cells in humanized mouse models may provide more evidence of their cytokine production characteristics.

sFv-ε could significantly mitigate the auto-activation of T cells relative to CARs and mediate antigen-specific TCR-like signaling. Both human and murine conventional sFv-ε T cells displayed equivalent or superior antitumor efficacy with reduced cytokine production compared with 28ζ and BBζ CAR T cells. GPC3-specific 7sFv-ε T cells further improved the antitumor immunity while preserving low production of cytokines associated with CRS, suggesting that it could be an effective and safe therapeutic strategy for the treatment of solid tumors.

MATERIALS AND METHODS

Constructions of sFv-ε, 7sFv-ε, or CARs

The human anti-GPC3 sFv-ε construct was composed of the humanized sFv targeting human GPC3 (9F2) and CD3ε tethered by a linker. The 28ζ CAR construct was described previously.[51] The BBζ CAR construct was composed of 9F2 linked by the hinge and transmembrane region of the CD8a chain and intracellular 4-1BB and CD3ζ signaling domains in tandem. Human sFv-ε, 28ζ, or BBζ CAR was cloned into the lentiviral vector pRRLSIN for expression. The murine anti-GPC3 sFv-ε construct was composed of 9F2 and murine CD3ε tethered by a linker. The 7sFv-ε construct was generated by coupling the murine sFv-ε and IL7 via a 2A peptide sequence. The murine 28ζ or BBζ CAR construct contained 9F2 and other hinge or domains derived from mice. Murine sFv-ε, 7sFv-ε, or CAR was cloned into the retroviral vector pMSCV-IRES-GFP for expression.

Cell lines

Jurkat cells were obtained from the Chinese Academy of Sciences and transduced with lentivirus and cultured in RPMI 1640 medium (Gibco) with 10% fetal bovine serum (FBS; Gibco). PLC/PRF/5 and SK-HEP-1 cells were obtained from the American Type Culture Collection. Hepa 1-6 cells were obtained from the Chinese Academy of Sciences and E0771 cells were conserved by our laboratory. Hepa 1-6 and E0771 were modified to express human-mouse chimeric GPC3, as previously reported.[35] All HCC and E0771 cells were cultivated in DMEM (Gibco) with 10% FBS, 100 U/mL penicillin, and 100μg/mL streptomycin (Invitrogen).

Generation of primary sFv-ε or CAR T cells

Peripheral blood mononuclear cells derived from healthy donors were provided by the Shanghai Blood Center. Human T cells were activated with anti-human CD3/CD28 beads (Invitrogen) for 48 h and transduced with lentivirus and cultured in AIM-V medium (Gibco) with 2% human serum type AB (Gemini) and 300 U/mL recombinant human IL2 (Shanghai Huaxin High Biotech). Murine T cells were isolated from spleen using the mouse T cell isolation kit (STEMCELL Technologies) and activated with anti-mouse CD3/CD28 beads (Gibco) for 24 h. Then, T cells were transduced with retrovirus and cultivated in RPMI 1640 medium containing 10% heat-inactivated FBS, 50μM 2-mercaptoethanol, and 100 U/mL recombinant human IL2.

Flow cytometry

9F2 on T cells was evaluated using biotin-conjugated GPC3 peptide (CARsgen Therapeutics) or biotin-conjugated goat anti-human Fab antibody (Jackson ImmunoResearch) with phycoerythrin (PE)-conjugated streptavidin. To measure calcium flux in T cells, T cells were loaded with Fluo-4 AM (Beyotime) and PLC/PRF/5 cells were labeled with CellTrace Violet dye (Thermo Fisher Scientific) in prior. After coculture with PLC/PRF/5 cells for different durations, CellTrace violet-negative T cells were evaluated by flow cytometry.

Figure 6. 7sFv-ε T cell therapy improved T cell persistence and immunological memory

(A and B) Tumor tissues were harvested 7 days after T cell infusion. Representative immunostaining images and quantification of tumor infiltrating T cells were shown (n = 6 shots from 3 different mice). Scale bars, 50μm. (C) Retroviral vector copy number in genomic DNA of tumor tissues (n = 3). (D) Expression of granzyme B in $CD8^+$ cells were analyzed in the single-cell suspensions of tumors by flow cytometry (n = 3). (E) Spleens were harvested 7 days after treatment. The $9F2^+$ T cells in spleens were analyzed by flow cytometry (n = 3). (F and G) Frequencies of $CD44^+$ $CD62L^+$ TCM subsets in $CD8^+$ T cells were analyzed in splenic $CD3^+$ T cells. (H and I) The draining lymph nodes were harvested 7 days after treatment. Frequencies of TCM subsets of $CD8^+$ T cells in lymph nodes were analyzed (n = 3). (J) Schematic diagram of re-challenge experiment. A total of 65 days after the first tumor inoculation, the tumor-rejected mice treated with 7sFv-ε T cells were rechallenged with 1×10^7 Hepa 1-6-GPC3 cells. As control, naive mice of the same age were also inoculated with tumors. (K) Tumor growth was assessed (n = 6). Data are represented as means ± SEMs. Statistical analysis was performed using one-way ANOVA followed by Tukey's test comparing engineered T cell groups against one another (B–E, G, I). *Adjusted $p \leq 0.05$, **adjusted $p \leq 0.01$, ***adjusted $p \leq 0.001$.

To analyze tumor-infiltrating T cells, tumor tissues were dissociated into single-cell suspensions by mechanical disruption and digestion with mixed enzyme solution. Cells were stained with anti-mouse CD45 APC (559864, BD Biosciences), anti-mouse CD8a PerCP/Cy5.5 (100734, BioLegend), and anti-mouse Granzyme B PE-eFluor 610 (61-8898-82, BioLegend) antibodies. The other antibodies were used as follows ("h" prefix denoting anti-human and "m" prefix denoting anti-mouse): hCD25 BV421 (562442, BD Biosciences), hCD69 APC (560967, BD Biosciences), hCD8 BV510 (563919, BD Biosciences), hCD45RA FITC (11-0458-42, Invitrogen), hCCR7 PE-CF594 (562381, BD Biosciences), hPD-1 BV421 (564323, BD Biosciences), hLAG-3 eFlour450 (48-2239-42, Invitrogen), mCD62L APC (553152, BD Biosciences), mCD44 BV510 (563114, BD Biosciences), mPD-1 BV421(562584, BD Biosciences), mLAG-3 APC (17-2231-82, Invitrogen), mCD3ε APC (100312, BioLegend), and mCD4 APC (561091, BD Biosciences).

Immunopurification and western blotting

Jurkat cells 2×10^7 were lysed with 1 mL lysis buffer for western blot/immunoprecipitation (WB/IP) assays (Absin) with phosphatase inhibitor cocktail and 1 mM PMSF for 30 min at 4°C. For the anti-9F2 immunoprecipitation, 500μL cleared cell lysate was incubated with 20μg biotin-conjugated GPC3 peptide and 6μL paramagnetic streptavidin-coupled beads (STEMCELL Technologies) for 2 h at 4°C. The immunoprecipitated material was subjected to 10% reducing SDS-PAGE. After being blotted onto polyvinylidene fluoride PVDF membrane, the protein of interest was detected by primary antibodies: hTCRα (515719, Santa Cruz), hTCRβ (79485, CST), hCD3γ (134096, Abcam), hCD3δ (109531, Abcam), hCD3ε (MA5-14524, Invitrogen), hCD3ζ (551034, BD Biosciences) and followed by incubation with horseradish peroxidase (HRP)-coupled anti-mouse immunoglobulin G (IgG) or HRP-coupled anti-rabbit IgG. To analyze TCR signaling, human T cells were starved overnight and stimulated with immobilized GPC3 peptide. This reaction was stopped by adding equal volume cold 2× lysis buffer (4% NP40, 50 mM Tris-HCl pH 7.4, 150 mM NaCl, 10 mM EDTA, 4 mM Na_3VO_4, 40 mM NaF, and protease inhibitor cocktail). To detect the apoptosis-related proteins, murine T cells cultured without IL2 for 24 h were lysed in T-PER Tissue Protein Extraction Reagent (Thermo Fisher Scientific) with protease inhibitor cocktail, 5 mM NaF, and 1 mM Na_3VO_4. The protein of interest was detected by primary antibodies: hCD3ζ-pY142 (558402, BD Biosciences), phospho-Zap-70 (Tyr319) (2717, CST), phospho-PLCγ1 (Tyr783) (14008, CST), phospho-NF-κB p65 (Ser536) (3033, CST), phospho-Akt (Ser473) (4060, CST), phospho-S6 ribosomal protein (Ser235/236) (4857, CST), glyceraldehyde 3-phosphate dehydrogenase (GAPDH) (KC-5G4, Aksomics), Mcl-1 (5453, CST), Bcl-xL (2764, CST), Survivin (2808, CST), Cleaved caspase 3 (9664, CST), and β-actin (4967, CST), followed by secondary antibodies.

In vitro cytotoxicity assays

T cells were cocultured with tumor cells at effector-to-target ratios of 1:1 and 1:3 for 18 h. The cytotoxicity of T cells was analyzed by the lactate dehydrogenase release in the supernatants using the Cytotoxicity Detection Kit (Roche).

Cytokine measurements

Human T cells 1×10^4 were cocultured with 1×10^4 PLC/PRF/5 cells with or without 1×10^4 monocytes in 200μL RPMI 1640 medium with 10% FBS for 48 h; 1×10^4 human T cells were activated with 1×10^4 PLC/PRF/5 cells with or without 0.25 nM FK506 for 8 h; and 1×10^4 murine T cells were cocultured with 1×10^4 Hepa 1-6-GPC3 cells for 20 h. Tumor mass was homogenized in T-PER Tissue Protein Extraction Reagent with protease inhibitor cocktail and the supernatants were collected after centrifugation. Cytokines in coculture supernatants or plasma or tumor mass were measured using cytometric bead arrays (CBA; BD Biosciences) for IFNγ, TNFα, IL2, and IL6 or ELISA kits (MultiSciences Biotechnology) for GM-CSF or IL7 according to the manufacturer's instructions.

RNA sequencing (RNA-seq) analysis

T cells were stimulated with plate-bound GPC3 peptide for 4 h. Total RNA was extracted using the RNeasy Mini Kit (Qiagen). Sequencing libraries were generated using VAHTS Stranded mRNA-seq Library Prep Kit for Illumina V2 (Vazyme). The sequencing was performed on an Illumina Nova seq platform and analyzed at Shanghai Biochip Corporation. RNA-seq count data were quantified as transcripts per million (TPM), which were then normalized using limma and visualized with pheatmap package in R between sFv-ε, 28ζ, and BBζ CAR T cells. GSEA of the calcium ion-related gene lists from MSigDB (C2 and C5) was performed by TPM (sFv-ε versus 28ζ CAR, sFv-ε vs BBζ CAR).

In vivo animal experiment

All of the animal studies were performed in accordance with the Experiment Animal Care Commission of the Shanghai Cancer Institute. Female immunodeficient mice (NOD-Prkdc^{scid} Il2rg^{null}, NPG) or C57BL/6 mice were housed under specific pathogen-free conditions. PLC/PRF/5 models were established by subcutaneous injection of 3×10^6 tumor cells in NPG mice. Mice were randomized into four treatment groups with the average tumor volume of 155 mm^3 and treated with an intravenous injection of 3×10^6 9F2$^+$ or UTD T cells. For Hepa 1-6-GPC3 models, 1×10^7 tumor cells were injected in the right flank of C57BL/6 mice. Mice were randomized into five groups with the average tumor volume of 170 mm^3 and treated with 1×10^6 T cells. For E0771-GPC3 models, 1×10^6 tumor cells were inoculated *in situ* in the C57BL/6 mammary gland. When the average tumor volume achieved 100 mm^3, mice were infused with 2×10^6 T cells. In the re-challenge experiment, after the tumors were eradicated by 7sFv-ε T cells, mice were re-injected with 1×10^7 Hepa 1-6-GPC3 cells in the contralateral flank. Tumor dimensions and body weight were measured every 2–5 days. Tumor volume was calculated by the formula $V= (length\times width^2)/2$.

Immunohistochemistry and RNA scope analysis

Tumor tissues and organs were fixed with formalin and embedded in paraffin and sectioned at a 5-μm thickness. The organs were stained with hematoxylin and eosin. The tumor tissue sections were stained with mCD8a (98941, CST) or mCD4 (183685, Abcam). The results were visualized using the Dako REAL EnVision Detection System. RNA *in situ* hybridization was performed using the RNAscope 2.5

HD Detection kit (Advanced Cell Diagnostics [ACD]) according to the manufacturer's instructions. The tumor tissue sections were deparaffinized and dehydrated and the endogenous peroxidase activity was quenched. After applying target retrieval reagents and Protease Plus, the sections were hybridized with probes targeting RNA-seq encoding 9F2 (501711, ACD) and Amplifier 1–6. Chromogenic detection was performed using the mixture of RED-A and RED-B followed by counterstaining with hematoxylin. Slides were scanned using NanoZoomer S360 (Hamamatsu), and the results were analyzed by NDP.view2 software (Hamamatsu).

Statistical analysis

All of the statistical analyses were performed using GraphPad Prism (version 8.4.3). One-way ANOVA followed by Tukey's or Dunnett's multiple comparison test were performed to assess differences between groups or differences between each group and the indicated control. Survival curves were analyzed using the log-rank test. Data are presented as means ± SEMs.

DATA AVAILABILITY

The data that support the findings of this study are available from the corresponding author upon reasonable request. Gene expression data from RNA-seq analysis were deposited in the NCBI Gene Expression Omnibus (GEO) database (GEO: GSE189932).

SUPPLEMENTAL INFORMATION

Supplemental information can be found online at https://doi.org/10.1016/j.omto.2022.04.003.

ACKNOWLEDGMENTS

This work was supported by the National Natural Science Foundation of China (nos. 82073359, 82073358, 81871918, and 81872483).

AUTHOR CONTRIBUTIONS

Z.L. and H.J. designed sFv-ε constructs and supervised the research. Y.S. and Y.D. designed and performed the experiments and wrote the manuscript. R.S., Y.W., H.L., and B.S. performed the experiments and analyzed the data. Y.L. analyzed the RNA-seq data and contributed to writing the manuscript.

DECLARATION OF INTERESTS

The authors declare no competing interests.

REFERENCES

1. Morgan, R.A., Dudley, M.E., Wunderlich, J.R., Hughes, M.S., Yang, J.C., Sherry, R.M., Royal, R.E., Topalian, S.L., Kammula, U.S., Restifo, N.P., et al. (2006). Cancer regression in patients after transfer of genetically engineered lymphocytes. Science *314*, 126–129. https://doi.org/10.1126/science.1129003.

2. Marincola, F.M., Jaffee, E.M., Hicklin, D.J., and Ferrone, S. (2000). Escape of human solid tumors from T-cell recognition: molecular mechanisms and functional significance. Adv. Immunol. *74*, 181–273. https://doi.org/10.1016/s0065-2776(08)60911-6.

3. Eshhar, Z., Waks, T., Gross, G., and Schindler, D.G. (1993). Specific activation and targeting of cytotoxic lymphocytes through chimeric single chains consisting of antibody-binding domains and the gamma or zeta subunits of the immunoglobulin and T-cell receptors. Proc. Natl. Acad. Sci. U S A *90*, 720–724. https://doi.org/10.1073/pnas.90.2.720.

4. Maher, J., Brentjens, R.J., Gunset, G., Riviere, I., and Sadelain, M. (2002). Human T-lymphocyte cytotoxicity and proliferation directed by a single chimeric TCRzeta /CD28 receptor. Nat. Biotechnol. *20*, 70–75. https://doi.org/10.1038/nbt0102-70.

5. Imai, C., Mihara, K., Andreansky, M., Nicholson, I.C., Pui, C.H., Geiger, T.L., and Campana, D. (2004). Chimeric receptors with 4-1BB signaling capacity provoke potent cytotoxicity against acute lymphoblastic leukemia. Leukemia *18*, 676–684. https://doi.org/10.1038/sj.leu.2403302.

6. Locke, F.L., Ghobadi, A., Jacobson, C.A., Miklos, D.B., Lekakis, L.J., Oluwole, O.O., Lin, Y., Braunschweig, I., Hill, B.T., Timmerman, J.M., et al. (2019). Long-term safety and activity of axicabtagene ciloleucel in refractory large B-cell lymphoma (ZUMA-1): a single-arm, multicentre, phase 1-2 trial. Lancet Oncol. *20*, 31–42. https://doi.org/10.1016/s1470-2045(18)30864-7.

7. Jain, P., Nastoupil, L., Westin, J., Lee, H.J., Navsaria, L., Steiner, R.E., Ahmed, S., Moghrabi, O., Oriabure, O., Chen, W., et al. (2021). Outcomes and management of patients with mantle cell lymphoma after progression on brexucabtagene autoleucel therapy. Br. J. Haematol. *192*, e38–e42. https://doi.org/10.1111/bjh.17197.

8. Jagannath, S., Lin, Y., Goldschmidt, H., Reece, D., Nooka, A., Senin, A., Rodriguez-Otero, P., Powles, R., Matsue, K., Shah, N., et al. (2021). KarMMa-RW: comparison of idecabtagene vicleucel with real-world outcomes in relapsed and refractory multiple myeloma. Blood Cancer J. *11*, 116. https://doi.org/10.1038/s41408-021-00507-2.

9. Schuster, S.J., Bishop, M.R., Tam, C.S., Waller, E.K., Borchmann, P., McGuirk, J.P., Jager, U., Jaglowski, S., Andreadis, C., Westin, J.R., et al. (2019). Tisagenlecleucel in adult relapsed or refractory diffuse large B-cell lymphoma. N. Engl. J. Med. *380*, 45–56. https://doi.org/10.1056/nejmoa1804980.

10. Abramson, J.S., Palomba, M.L., Gordon, L.I., Lunning, M.A., Wang, M., Arnason, J., Mehta, A., Purev, E., Maloney, D.G., Andreadis, C., et al. (2020). Lisocabtagene maraleucel for patients with relapsed or refractory large B-cell lymphomas (TRANSCEND NHL 001): a multicentre seamless design study. Lancet *396*, 839–852. https://doi.org/10.1016/s0140-6736(20)31366-0.

11. Davila, M.L., Riviere, I., Wang, X., Bartido, S., Park, J., Curran, K., Chung, S.S., Stefanski, J., Borquez-Ojeda, O., Olszewska, M., et al. (2014). Efficacy and toxicity management of 19-28z CAR T cell therapy in B cell acute lymphoblastic leukemia. Sci. Transl. Med. *6*, 224ra25. https://doi.org/10.1126/scitranslmed.3008226.

12. Berdeja, J.G., Madduri, D., Usmani, S.Z., Jakubowiak, A., Agha, M., Cohen, A.D., Stewart, A.K., Hari, P., Htut, M., Lesokhin, A., et al. (2021). Ciltacabtagene autoleucel, a B-cell maturation antigen-directed chimeric antigen receptor T-cell therapy in patients with relapsed or refractory multiple myeloma (CARTITUDE-1): a phase 1b/2 open-label study. Lancet *398*, 314–324. https://doi.org/10.1016/s0140-6736(21)00933-8.

13. Schaft, N. (2020). The landscape of CAR-T cell clinical trials against solid tumors-A comprehensive overview. Cancers (Basel) *12*, 2567. https://doi.org/10.3390/cancers12092567.

14. Alcantara, M., Du Rusquec, P., and Romano, E. (2020). Current clinical evidence and potential solutions to increase benefit of CAR T-cell therapy for patients with solid tumors. Oncoimmunology *9*, 1777064. https://doi.org/10.1080/2162402x.2020.1777064.

15. Marofi, F., Motavalli, R., Safonov, V.A., Thangavelu, L., Yumashev, A.V., Alexander, M., Shomali, N., Chartrand, M.S., Pathak, Y., Jarahian, M., et al. (2021). CAR T cells in solid tumors: challenges and opportunities. Stem Cell Res. Ther. *12*, 81. https://doi.org/10.1186/s13287-020-02128-1.

16. Pilon-Thomas, S., Kuhn, L., Ellwanger, S., Janssen, W., Royster, E., Marzban, S., Kudchadkar, R., Zager, J., Gibney, G., Sondak, V.K., et al. (2012). Efficacy of adoptive cell transfer of tumor-infiltrating lymphocytes after lymphopenia induction for metastatic melanoma. J. Immunother. *35*, 615–620. https://doi.org/10.1097/cji.0b013e31826e8f5f.

17. Robbins, P.F., Morgan, R.A., Feldman, S.A., Yang, J.C., Sherry, R.M., Dudley, M.E., Wunderlich, J.R., Nahvi, A.V., Helman, L.J., Mackall, C.L., et al. (2011). Tumor regression in patients with metastatic synovial cell sarcoma and melanoma using genetically engineered lymphocytes reactive with NY-ESO-1. J. Clin. Oncol. *29*, 917–924. https://doi.org/10.1200/jco.2010.32.2537.

18. Robbins, P.F., Kassim, S.H., Tran, T.L.N., Crystal, J.S., Morgan, R.A., Feldman, S.A., Yang, J.C., Dudley, M.E., Wunderlich, J.R., Sherry, R.M., et al. (2015). A pilot trial using lymphocytes genetically engineered with an NY-ESO-1-Reactive T-cell

receptor: long-term follow-up and correlates with response. Clin. Cancer Res. *21*, 1019–1027. https://doi.org/10.1158/1078-0432.ccr-14-2708.

19. Nolan, K.F., Yun, C.O., Akamatsu, Y., Murphy, J.C., Leung, S.O., Beecham, E.J., and Junghans, R.P. (1999). Bypassing immunization: optimized design of "designer T cells" against carcinoembryonic antigen (CEA)-expressing tumors, and lack of suppression by soluble CEA. Clin. Cancer Res. *5*, 3928–3941.
20. Gao, H., Li, K., Tu, H., Pan, X., Jiang, H., Shi, B., Kong, J., Wang, H., Yang, S., Gu, J., and Li, Z. (2014). Development of T cells redirected to glypican-3 for the treatment of hepatocellular carcinoma. Clin. Cancer Res. *20*, 6418–6428. https://doi.org/10.1158/1078-0432.ccr-14-1170.
21. Moek, K.L., Fehrmann, R.S.N., van der Vegt, B., de Vries, E.G.E., and de Groot, D.J.A. (2018). Glypican 3 overexpression across a broad spectrum of tumor types discovered with functional genomic mRNA profiling of a large cancer database. Am. J. Pathol. *188*, 1973–1981. https://doi.org/10.1016/j.ajpath.2018.05.014.
22. Shi, D., Shi, Y., Kaseb, A.O., Qi, X., Zhang, Y., Chi, J., Lu, Q., Gao, H., Jiang, H., Wang, H., et al. (2020). Chimeric antigen receptor-glypican-3 T-cell therapy for advanced hepatocellular carcinoma: results of phase I trials. Clin. Cancer Res. *26*, 3979–3989. https://doi.org/10.1158/1078-0432.ccr-19-3259.
23. Fuca, G., Reppel, L., Landoni, E., Savoldo, B., and Dotti, G. (2020). Enhancing chimeric antigen receptor T-cell efficacy in solid tumors. Clin. Cancer Res. *26*, 2444–2451. https://doi.org/10.1158/1078-0432.ccr-19-1835.
24. Walsh, S.R., Simovic, B., Chen, L., Bastin, D., Nguyen, A., Stephenson, K., Mandur, T.S., Bramson, J.L., Lichty, B.D., and Wan, Y. (2019). Endogenous T cells prevent tumor immune escape following adoptive T cell therapy. J. Clin. Invest. *129*, 5400–5410. https://doi.org/10.1172/jci126199.
25. Colombetti, S., Levy, F., and Chapatte, L. (2009). IL-7 adjuvant treatment enhances long-term tumor-antigen-specific CD8+ T-cell responses after immunization with recombinant lentivector. Blood *113*, 6629–6637. https://doi.org/10.1182/blood-2008-05-155309.
26. Nanjappa, S.G., Walent, J.H., Morre, M., and Suresh, M. (2008). Effects of IL-7 on memory CD8 T cell homeostasis are influenced by the timing of therapy in mice. J. Clin. Invest. *118*, 1027–1039. https://doi.org/10.1172/JCI32020.
27. Luo, H., Su, J., Sun, R., Sun, Y., Wang, Y., Dong, Y., Shi, B., Jiang, H., and Li, Z. (2020). Coexpression of IL7 and CCL21 increases efficacy of CAR-T cells in solid tumors without requiring preconditioned lymphodepletion. Clin. Cancer Res. *26*, 5494–5505. https://doi.org/10.1158/1078-0432.ccr-20-0777.
28. Adachi, K., Kano, Y., Nagai, T., Okuyama, N., Sakoda, Y., and Tamada, K. (2018). IL-7 and CCL19 expression in CAR-T cells improves immune cell infiltration and CAR-T cell survival in the tumor. Nat. Biotechnol. *36*, 346–351. https://doi.org/10.1038/nbt.4086.
29. Calderon, H., Mamonkin, M., and Guedan, S. (2020). Analysis of CAR-mediated tonic signaling. Methods Mol. Biol. *2086*, 223–236. https://doi.org/10.1007/978-1-0716-0146-4_17.
30. Ajina, A., and Maher, J. (2018). Strategies to address chimeric antigen receptor tonic signaling. Mol. Cancer Ther. *17*, 1795–1815. https://doi.org/10.1158/1535-7163.mct-17-1097.
31. Norelli, M., Camisa, B., Barbiera, G., Falcone, L., Purevdorj, A., Genua, M., Sanvito, F., Ponzoni, M., Doglioni, C., Cristofori, P., et al. (2018). Monocyte-derived IL-1 and IL-6 are differentially required for cytokine-release syndrome and neurotoxicity due to CAR T cells. Nat. Med. *24*, 739–748. https://doi.org/10.1038/s41591-018-0036-4.
32. Savignac, M., Mellstrom, B., and Naranjo, J.R. (2007). Calcium-dependent transcription of cytokine genes in T lymphocytes. Pflugers Arch. *454*, 523–533. https://doi.org/10.1007/s00424-007-0238-y.
33. Klein-Hessling, S., Muhammad, K., Klein, M., Pusch, T., Rudolf, R., Floter, J., Qureischi, M., Beilhack, A., Vaeth, M., Kummerow, C., et al. (2017). NFATc1 controls the cytotoxicity of CD8(+) T cells. Nat. Commun. *8*, 511. https://doi.org/10.1038/s41467-017-00612-6.
34. Andersson, J., Nagy, S., Groth, C.G., and Andersson, U. (1992). Effects of FK506 and cyclosporin A on cytokine production studied in vitro at a single-cell level. Immunology *75*, 136–142.
35. Wu, X., Luo, H., Shi, B., Di, S., Sun, R., Su, J., Liu, Y., Li, H., Jiang, H., and Li, Z. (2019). Combined antitumor effects of sorafenib and GPC3-CAR T cells in mouse models of hepatocellular carcinoma. Mol. Ther. *27*, 1483–1494. https://doi.org/10.1016/j.ymthe.2019.04.020.
36. Ewens, A., Luo, L., Berleth, E., Alderfer, J., Wollman, R., Hafeez, B.B., Kanter, P., Mihich, E., and Ehrke, M.J. (2006). Doxorubicin plus interleukin-2 chemoimmunotherapy against breast cancer in mice. Cancer Res. *66*, 5419–5426. https://doi.org/10.1158/0008-5472.can-05-3963.
37. Helsen, C.W., Hammill, J.A., Lau, V.W.C., Mwawasi, K.A., Afsahi, A., Bezverbnaya, K., Newhook, L., Hayes, D.L., Aarts, C., Bojovic, B., et al. (2018). The chimeric TAC receptor co-opts the T cell receptor yielding robust anti-tumor activity without toxicity. Nat. Commun. *9*, 3049. https://doi.org/10.1038/s41467-018-05395-y.
38. Baeuerle, P.A., Ding, J., Patel, E., Thorausch, N., Horton, H., Gierut, J., Scarfo, I., Choudhary, R., Kiner, O., Krishnamurthy, J., et al. (2019). Synthetic TRuC receptors engaging the complete T cell receptor for potent anti-tumor response. Nat. Commun. *10*, 2087. https://doi.org/10.1038/s41467-019-10097-0.
39. Ando, M., Ito, M., Srirat, T., Kondo, T., and Yoshimura, A. (2020). Memory T cell, exhaustion, and tumor immunity. Immunol. Med. *43*, 1–9. https://doi.org/10.1080/25785826.2019.1698261.
40. Mazzucchelli, R., and Durum, S.K. (2007). Interleukin-7 receptor expression: intelligent design. Nat. Rev. Immunol. *7*, 144–154. https://doi.org/10.1038/nri2023.
41. Sportes, C., Babb, R.R., Krumlauf, M.C., Hakim, F.T., Steinberg, S.M., Chow, C.K., Brown, M.R., Fleisher, T.A., Noel, P., Maric, I., et al. (2010). Phase I study of recombinant human interleukin-7 administration in subjects with refractory malignancy. Clin. Cancer Res. *16*, 727–735. https://doi.org/10.1158/1078-0432.ccr-09-1303.
42. Pang, N., Shi, J., Qin, L., Chen, A., Tang, Y., Yang, H., Huang, Y., Wu, Q., Li, X., He, B., et al. (2021). IL-7 and CCL19-secreting CAR-T cell therapy for tumors with positive glypican-3 or mesothelin. J. Hematol. Oncol. *14*, 118. https://doi.org/10.1186/s13045-021-01128-9.
43. Kaech, S.M., Tan, J.T., Wherry, E.J., Konieczny, B.T., Surh, C.D., and Ahmed, R. (2003). Selective expression of the interleukin 7 receptor identifies effector CD8 T cells that give rise to long-lived memory cells. Nat. Immunol. *4*, 1191–1198. https://doi.org/10.1038/ni1009.
44. Sportes, C., Hakim, F.T., Memon, S.A., Zhang, H., Chua, K.S., Brown, M.R., Fleisher, T.A., Krumlauf, M.C., Babb, R.R., Chow, C.K., et al. (2008). Administration of rhIL-7 in humans increases in vivo TCR repertoire diversity by preferential expansion of naive T cell subsets. J. Exp. Med. *205*, 1701–1714. https://doi.org/10.1084/jem.20071681.
45. Hooijberg, E., Bakker, A.Q., Ruizendaal, J.J., and Spits, H. (2000). NFAT-controlled expression of GFP permits visualization and isolation of antigen-stimulated primary human T cells. Blood *96*, 459–466. https://doi.org/10.1182/blood.v96.2.459.014k50_459_466.
46. Roybal, K.T., Williams, J.Z., Morsut, L., Rupp, L.J., Kolinko, I., Choe, J.H., Walker, W.J., McNally, K.A., and Lim, W.A. (2016). Engineering T cells with customized therapeutic response programs using synthetic notch receptors. Cell *167*, 419–432.e16. https://doi.org/10.1016/j.cell.2016.09.011.
47. Giavridis, T., van der Stegen, S.J.C., Eyquem, J., Hamieh, M., Piersigilli, A., and Sadelain, M. (2018). CAR T cell-induced cytokine release syndrome is mediated by macrophages and abated by IL-1 blockade. Nat. Med. *24*, 731–738. https://doi.org/10.1038/s41591-018-0041-7.
48. Zhou, X., Friedmann, K.S., Lyrmann, H., Zhou, Y., Schoppmeyer, R., Knorck, A., Mang, S., Hoxha, C., Angenendt, A., Backes, C.S., et al. (2018). A calcium optimum for cytotoxic T lymphocyte and natural killer cell cytotoxicity. J. Physiol. *596*, 2681–2698. https://doi.org/10.1113/jp274964.
49. Faroudi, M., Utzny, C., Salio, M., Cerundolo, V., Guiraud, M., Muller, S., and Valitutti, S. (2003). Lytic versus stimulatory synapse in cytotoxic T lymphocyte/target cell interaction: manifestation of a dual activation threshold. Proc. Natl. Acad. Sci. U S A *100*, 14145–14150. https://doi.org/10.1073/pnas.2334336100.
50. Wu, W., Zhou, Q., Masubuchi, T., Shi, X., Li, H., Xu, X., Huang, M., Meng, L., He, X., Zhu, H., et al. (2020). Multiple signaling roles of CD3ε and its application in CAR-T cell therapy. Cell *182*, 855–871.e23. https://doi.org/10.1016/j.cell.2020.07.018.
51. Yu, M., Luo, H., Fan, M., Wu, X., Shi, B., Di, S., Liu, Y., Pan, Z., Jiang, H., and Li, Z. (2018). Development of GPC3-specific chimeric antigen receptor-engineered natural killer cells for the treatment of hepatocellular carcinoma. Mol. Ther. *26*, 366–378. https://doi.org/10.1016/j.ymthe.2017.12.012.